Linagliptin, a xanthine-based dipeptidyl peptidase-4 inhibitor, ameliorates experimental autoimmune myocarditis by suppressing cathepsin-G activity

Yuka Shiheido-Watanabe
Tokyo Medical and Dental University Graduate School of Medical and Dental Sciences: Tokyo Ika Shika Daigaku Daigakin Ishigaku Sogo Kenkyuka

Yasuhiro Maejima (ymaeji.cvm@tmd.ac.jp)
Tokyo Ika Shika Daigaku Daigakin Ishigaku Sogo Kenkyuka https://orcid.org/0000-0001-7450-4840

Shun Nakagama
Tokyo Medical and Dental University Graduate School of Medical and Dental Sciences: Tokyo Ika Shika Daigaku Daigakin Ishigaku Sogo Kenkyuka

Natsuko Tamura
Tokyo Medical and Dental University Faculty of Medicine: Tokyo Ika Shika Daigaku Daigakin Ishigaku Sogo Kenkyuka

Takeshi Kasama
Tokyo Kogyo Daigaku Daigakuin Sogo Rikogaku Kenkyuka

Tetsuo Sasano
Tokyo Medical and Dental University Graduate School of Medical and Dental Sciences: Tokyo Ika Shika Daigaku Daigakin Ishigaku Sogo Kenkyuka

Original investigation

Keywords: Dipeptidyl peptidase-4, Autoimmune Myocarditis, Inflammation, Heart failure

Posted Date: September 14th, 2020

DOI: https://doi.org/10.21203/rs.3.rs-70009/v1

Abstract

Background

There is a compelling need for establishing effective therapy for autoimmune myocarditis which primarily manifest as chest pain, heart failure or sudden death. Although our group have previously shown that dipeptidyl peptidase-4 (DPP-4) aggravates experimental autoimmune myocarditis (EAM), the detailed underlying mechanism remains to be unelucidated.

Methods

The effects of linagliptin, a xanthine-based dipeptidyl peptidase-4 inhibitor, on cardiac function were investigated by treating mouse EAM models and elucidated the role of DPP-4 on EAM using proteomic approaches.

Results

Immunohistochemical analyses demonstrated that the number of Th17 cells expressing high level of DPP-4 infiltrated to EAM myocardium was significantly attenuated by linagliptin treatment. MS/MS-based analyses demonstrated that DPP-4 binds to cathepsin-G in EAM hearts. DPP-4 also protects cathepsin-G activity by inhibiting the activity of SerpinA3N, a protease inhibitor that catalyzes cathepsin-G. The activity of cathepsin-G and the level of Angiotensin II were markedly elevated in EAM myocardium; this effect was reversed by linagliptin treatment. Furthermore, we found that linagliptin suppresses oxidative stress in EAM hearts.

Conclusions

DPP-4 physically interacts with cathepsin-G, which, in turn, suppresses SerpinA3N; this promotes angiotensin II accumulation in EAM hearts. Thus, DPP-4 derived from Th17 cells could aggravate cardiac dysfunction during EAM.

Background

Myocarditis is the leading cause of non-hereditary heart failure developing at a young age (< 40-year old) [1]. Among myocarditis patients that were diagnosed by histological evidence with a myocardial biopsy, 10–20% patients will develop to dilated cardiomyopathy [2]. The frequency of autoimmunity-mediated myocarditis is relatively low compared to that of infection-mediated myocarditis. However, it is important to identify the cause of myocarditis to choose effective therapeutic strategies including immunosuppressive therapy. Additionally, recently, autoimmune myocarditis was identified as a serious side effect of immune checkpoint inhibitors, a novel category of anti-cancer drugs that help direct the

immune system to recognize and target cancer cells [3, 4]. Thus, it is imperative to identify mechanisms leading to myocarditis based on autoimmune abnormalities and develop effective therapies.

Dipeptidyl peptidase-4 (DPP-4) is a membrane glycoprotein of 110 kDa and a serine protease that cleaves X-proline/alanine dipeptides from the N-terminus of polypeptides. The most well-known substrates of DPP-4 are incretins such as glucagon-like peptide-1 (GLP-1) and glucose-dependent insulintropic polypeptide (GIP). When DPP-4 is inhibited, blood levels of incretins are raised and act on both pancreatic islet cell types, thereby promoting hypoglycemic action in those cells. Currently, DPP-4 inhibitors are the most widely used drugs in the treatment of diabetes because of their efficacy and safety for low incidence hypoglycemia. On the other hand, increasing lines of evidence suggest that DPP-4 is critical for the regulation of inflammatory responses [5].

DPP-4, also known as CD26, is expressed on the cell surface of T-lymphocytes and acts as a co-stimulatory pathway of T-lymphocytes; this pathway is involved in the regulation of the cell-mediated immune system [6]. Bengsch et al. demonstrated that an active form of CD26 is highly expressed on the cell surface of Th17 lymphocytes, a subtype of helper T-lymphocytes that are considered to be involved in the pathogenesis of autoimmune diseases [7]. In addition, Zhong et al. demonstrated that CD26 on dendritic cells/macrophages plays a critical role in promoting obesity-induced visceral inflammation [8]. These findings led us to hypothesize that inhibition of DPP-4 could be effective for the suppression of autoimmune myocarditis. Our group have previously demonstrated that linagliptin, a selective DPP-4 inhibitor that has a high degree of affinity for DPP-4 in various tissues [9–11], is useful in an experimental autoimmune myocarditis (EAM) model [12]. However, the precise mechanism through which linagliptin exerts its anti-inflammatory effect to suppress myocarditis remains to be elucidated.

In this study, we demonstrated that DPP-4 physically interacts with cathepsin-G, a plasma membrane-bound serine protease, in EAM mice hearts. Furthermore, we also present evidence suggesting that suppression of cathepsin-G activity by administration of linagliptin effectively attenuates myocardial inflammation by regulating the activities of both SerpinA3N and angiotensin II in EAM mice.

Materials And Methods

Experimental Animal Models of myocarditis

Male BALB/c mice (6 weeks of age, body weight: 20-25 g) were purchased from Japan Clea, Co. (Tokyo, Japan).

Experimental autoimmune myocarditis was induced in BALB/c mice by subcutaneous injection of the α-Myosin heavy chain (α-MyHC) peptides (150 μg per mouse) emulsified with Complete Freund's adjuvant on day 0 and 7. On day 0, 500 ng of pertussis toxin were also administrated intraperitoneally at the same time to induce the EAM mice model. EAM mice were assigned to one of the following two groups: EAM mice group treated with linagliptin (3 mg/kg) and untreated controls. Mice were sacrificed on Day 21. For

the experiments of Angiotensin II receptor type 1(AT1) blockade, losartan (LOS) (10 mg/kg/day; MERCK & Co., Inc., Kenilworth, NJ, USA) was given to the mice in their drinking water [13].

Echocardiography

A transthoracic echocardiography was performed on animals anesthetized by intraperitoneal administration of 3.6% chloral hydrate (Wako Pure Chemical Industries, Osaka, Japan) in saline (0.1 mL/10 g body weight). For the left ventricular echocardiographic recording, an echocardiographic machine with a 14-MHz transducer (Toshiba, Tokyo, Japan) was used. A two-dimensional targeted M-mode and B-mode echocardiogram was obtained along the short-axis view of the left ventricle at the level of the papillary muscles. Left ventricular end-diastolic (LVDd) and end-systolic (LVDs) dimensions and left ventricular fractional shortening (LVFS = ((LVDd − LVDs) / LVDd)) were calculated from M-mode echocardiograms over 3 consecutive cardiac cycles according to the American Society for Echocardiography leading edge method. The measurements of 3 consecutive cardiac cycles were averaged. Measurements were made offline by two independent investigators.

Histopathology

Hearts were harvested immediately after animals were sacrificed by cutting the abdominal aorta under deep anesthesia on day 21. After measuring the weight (mg), mid-ventricular slices of the heart were stained with hematoxylin and eosin (HE) and Mallory methods. Blue staining of collagen fibers was quantified as a measure of fibrosis using the Image-Pro Express software program. The average infarct size was obtained by calculating the area ratio (fibrosis area/entire area). The area of the myocardium affected by cell infiltration was determined as infiltrated. All data were analyzed in a blind fashion by two independent investigators and averaged.

Immunohistochemistry

Immunohistochemistry was performed to evaluate the amount of a thymus-specific isoform of the RAR-related orphan nuclear receptor gamma (RORγt), cathepsin G, and 8-hydroxyguanosine (8-OHdG), a marker of oxidative stress in DNA, in the hearts of mice on day 21. Frozen sections were fixed in acetone at 4^{o}C. The sections were incubated with unlabeled primary antibodies overnight at 4^{o}C and washed in PBS. The antibody-HRP conjugate was detected with a Histofine Simple Stain Kit (Nichirei Corporation, Tokyo, Japan), following the manufacturer's instructions. RORγt-positive cells were counted and the number was divided by the entire area.

DPP-4 activity assay

The activity of DPP-4 was evaluated in myocardium tissues using a DPP-4 activity assay kit (BioVision, Milpitas, CA) according to the manufacturer's instructions.

T cell proliferation assay

Spleen cells were isolated from mice with myocarditis on day 18. Cells (5×10^5/well) were cultured in 96-well plates with 50 μg/mL purified porcine heart myosin (Sigma, St. Louis, MO). Linagliptin was added to each well at various concentrations. Cells were incubated at 37 °C under 5% CO_2 for three days. T cell proliferation was assessed by MTT assay with Cell Counting Kit-8 (Dojindo, Tokyo, Japan). Cell proliferation was expressed as the optical density [14].

Protein extraction from the myocardium

Heart specimens, which were harvested immediately after mice were sacrificed on day 21, were homogenized in RIPA buffer (50 mM Tris-HCl, pH 7.6, 150 mM NaCl, 0.5% DOC, 0.1% SDS, 1% NP-40). Regarding the samples used for Tandem Mass Tag (TMT) labeling, heart specimens were homogenized in a Minute Plasma Membrane Protein Isolation Kit (Invent Biotechnologies, Inc.). Samples were centrifuged, and the supernatant was transferred to new tubes. Protein concentration was determined using a BCA protein assay (Pierce Biotechnology, Rockford, IL). Proteins were stored at −80°C until further analysis.

Immunoprecipitation

Human embryonic kidney 293 cells were cultured for 18 to 24 hours to approximately 80% confluence in 10 cm plates and then transfected with 10 ng of plasmid (Flag-DPP-4 or Flag-Empty) using FuGene6 (20 μL) (Roche, Basel, Switzerland), according to the manufacturer's instructions. After 48 hours of transfection, cells were harvested, and solubilized in a lysis buffer (50 mM Tris-HCl, pH 7.4, 1% Triton X-100, 150 mM NaCl, 1 mM phenylpethyl sulfonyl fluoride, 10 μg/mL aprotinin). Total cell lysates (500 μg) were immunoprecipitated with Flag antibody-conjugated magnetic beads overnight at 4°C. Immunoprecipitates were washed several times with lysis buffer.

TMT Labeling

Immunoprecipitates with Flag antibody-conjugated magnetic beads (described above) were incubated with heart lysates extracted with a Minute Plasma Membrane Protein Isolation Kit for 6 hours at 4°C. Cells were washed with 500 uL of TBS-T for 10 min at 4^{o}C five consecutive times. They were then added to the elution buffer (0.1 M glycine with HCl) and neutralized with 1 M Tris-HCl [pH 9.0]. TMT labeling was performed using TMT Mass Tagging Kits and Reagents (Thermo Scientific, Rockford, IL, U.S.A.) according to the manufacturer's instructions. The eluted proteins were adjusted to 100 μL with 100 mM TEAB; additionally, 5 μL of the 200 mM TCEP were added, and samples were incubated at 55°C for 1 hour. Then, 5 μL of 375 mM iodoacetamide were added to the sample and incubated for 30 minutes protected from light at room temperature. Trypsin was added (final concentration: 2.5%) to sample proteins in TEAB and samples were digested overnight at 37°C. As a labeling step, 41 μL of the TMT Label Reagent were added to each 100 μL sample. After incubating the reaction for 1 hour at room temperature, 8 μL of 5% hydroxylamine were added to the sample and incubated for 15 minutes to quench the reaction.

LC-MS/MS Analysis

The aliquot of TMT-labeled samples was analyzed using a LTQ Orbitrap Velos hybrid mass spectrometer (Thermo Scientific) equipped with an Easy nLC II nano-LC system (Proxeon, Denmark) and Chip-Mate nano-ESI interface unit (Advion Inc., U.S.A.). The Nano-LC column was a MonoCap C18 Nano-flow 100 μm i.d. × 750 mm (GL Sciences, Japan). Nano-LC settings were configured as follow: Flow rate was 300 nL/min. Water containing 0.1% formic acid was used as eluent A. Acetonitrile/water (7:3, v/v) containing 0.1% formic acid was used as eluent B. The gradient of eluent B was set as follows: 0% – 5 min – 20% – 45 min – 57% – 10 min. The acquired MS and MS/MS spectra were processed with Proteome Discoverer 1.3 Software (Thermo Scientific).

Cathepsin-G activity assay

The activity of cathepsin-G was evaluated in myocardium tissues and mixtures of recombinant mouse DPP-4 (R&D Systems, Minneapolis, MN), recombinant mouse SerpinA3N (R&D Systems), and cathepsin-G (Enzo Biochem, New York, NY) using a cathepsin-G Activity Assay Kit (Abcam, Cambridge, United Kingdom) according to the manufacturer's instructions. Briefly, the mixture of DPP-4, SerpinA3N, and cathepsin-G or the mixture of SerpinA3N and cathepsin-G was mixed with assay buffer and incubated at 37°C for 10 min. Then, the substrate solution (assay buffer and *p*-NA) was added to each well. Absorbance was detected at 405 nm using a microplate reader (Bio-Rad, Hercules, CA) at 0 min. A second read was performed after incubating the reaction at 37°C for 60 min, protected from light.

SerpinA3N activity assay

The activity of SerpinA3N was evaluated in mixtures of DPP-4 and SerpinA3N, and extracted proteins from the myocardium according to the manufacturer's instructions. The activity of SerpinA3N was measured by its ability to inhibit Granzyme B cleavage of *tert*-butoxycarbonyl-Ala-Ala-Asp-thiobenzyl ester (Boc-AAD-SBzl). Briefly, the mixture of DPP-4, SerpinA3N, and activated recombinant human Granzyme B (R&D Systems) or the mixture of Serpin A3N and Granzyme B was mixed with the assay buffer (50 mM Tris, pH 7.5). Then, the substrate mixture, which consisted of 5,5'-dithio-bis 2-nitrobenzoic acid (DTNB, Sigma-Aldrich, St. Louis, MO), Boc-AAD-SBzl (SM Biochemicals, Anaheim, CA), and assay buffer, was added to each well. The absorbance was detected at 405 nm in kinetic mode for 5 minutes using a microplate reader (Bio-Rad).

ELISA

Levels of Serpin A3N in homogenates of EAM hearts were determined by an ELISA using an immunoassay kit (Aviva Systems Biology, San Diego, CA, USA). The ELISA was performed according to the manufacturer's instructions.

Angiotensin II assay

The amount of Angiotensin II was evaluated in myocardium tissues using an Angiotensin II ELISA kit (Sigma) according to the manufacturer's instructions.

Chymase activity assay

Chymase activity was measured as described [15] Briefly, tissue extracts were incubated for 30 min at 37ºC with a substrate Suc-Ala-Ala-Pro-Phe-4-methylcoumaryl-7-amide (5 mmol/l; Fuji Film-Wako) in 100 mmol/l Tris-HCl buffer (pH 8.5, 200 mmol/l NaCl). After termination of the enzyme reaction by adding 3% metaphosphoric acid (w/v), the amount of 7-amino-4-methylcoumarin (AMC) was measured by fluorophotometric determination (excitation, 380 nm; emission, 460 nm). One unit of chymase activity was defined as the amount of enzyme that cleaved 1 μmol AMC/min.

Hydrogen peroxide assay

EAM heart tissues (day 21) were homogenized and sonicated in 50 mM potassium phosphate buffer and 0.5% hexadecyltrimethylammonium bromide (HTAB). Samples were centrifuged, and the supernatant was transferred to new tubes. The concentration of hydrogen peroxide was determined using a hydrogen peroxide colorimetric/fluorometric assay kit (BioVision) according to the manufacturer's instructions.

Statistics

All data are expressed as mean ± SEM. All statistical analyses were performed using an unpaired Student's *t*-test or One-Way ANOVA, followed by a post hoc Bonferroni-Dunn's comparison test for multiple group comparisons. A value of $P<0.05$ was considered to be significant.

Results

Treatment with linagliptin attenuates inflammatory cell infiltration and fibrosis in EAM hearts

Left ventricular systolic function, evaluated by echocardiographic examination, was significantly higher in linagliptin-treated EAM hearts than in untreated ones after 21 days of EAM induction (Figure 1A). Lung weight of linagliptin-treated EAM mice was significantly less than that of untreated ones (Figure 1B). Histopathologic examination revealed that inflammatory cell infiltration in EAM hearts was markedly attenuated by treatment with linagliptin after 21 days of EAM induction (Figure 1C); likewise, cardiac fibrosis after EAM induction was significantly decreased by treatment with linagliptin (Figure 1D). Taken together, these results suggest that linagliptin treatment effectively attenuates inflammatory cell infiltration and fibrosis in EAM hearts, thereby restoring cardiac dysfunction caused by EAM.

The increase in DPP-4 activity was significantly suppressed by linagliptin treatment in EAM hearts

We next elucidated the mechanism through which DPP-4 aggravates EAM. The activity of DPP-4 in EAM myocardial tissues was significantly elevated compared to those in control mice, and its activity was significantly suppressed by linagliptin treatment (Figure 2A). Increasing lines of evidence suggest that

EAM is transferable to other individuals via EAM-derived splenic T cells [16]. To examine the effect of linagliptin on antigen-induced T-cell proliferation, we conducted T-cell proliferation assay using EAM-derived splenocytes and found that treatment with linagliptin suppressed myosin-induced T-cell proliferation in a dose-dependent manner (Figure 2B).

It has been shown that Th17 cells express high levels of enzymatically active DPP-4, and enhance the immune response of Th17 cells through a chemotactic effect of DPP-4 [7]. To examine the effects of linagliptin on the number of Th17 cells in EAM, immunostaining was performed using a RORγt antibody, marker of Th17 cells. The number of Th17 cells infiltrating the myocardial tissue of EAM was markedly suppressed by linagliptin treatment (Figure 2C). We also found that DPP-4 was colocalized with RORγt in the infiltrating cells of the EAM hearts (Figure 2D).

These results indicate that the increase in DPP-4 activity was significantly suppressed by linagliptinreatment in EAM hearts, possibly through suppressing the number of RORγt-positive Th17 cells infiltrated to the EAM hearts.

DPP-4 physically interacts with cathepsin-G,a membrane-bound serine protease, in EAM hearts

In order to elucidate how DPP-4 contributes to the progression of EAM, proteins that interact with DPP-4 in EAM myocardial tissues were explored by a TMT method using mass spectrometric analyses. Specifically, we immunoprecipitated a homogenate of Flag-DPP-4 or Flag-empty proteins with EAM myocardial tissues and labeled each immunoprecipitate with a different probe to subtract the signal of nonspecific binding substances (Figure 3A). Using this technique, we found that cathepsin-G strongly interacts with DPP-4 (Figure 3B, C). Co-immunoprecipitation assays demonstrated that endogenous cathepsin-G strongly interacted with Flag-DPP-4 *in vivo* (Figure 3D). These results suggest that DPP-4 physically interacts with cathepsin-G in EAM hearts.

DPP-4 increases cathepsin G activity in EAM hearts

The activity of cathepsin-G in EAM hearts was significantly elevated; furthermore, linagliptin treatment suppressed DPP-4 activity and also cathepsin-G activity in EAM hearts (Figure 4A), suggesting that suppression of DPP-4 decreases cathepsin-G activity in EAM hearts. Based on these findings, DPP-4 could play a critical role on protecting cathepsin-G activity by binding with it. However, DPP-4 cannot directly regulate cathepsin-G activity, as cathepsin-G does not have X-proline/alanine dipeptides in its N-terminus. To resolve this conundrum, we speculated that DPP-4 inactivates cathepsin-G-suppressing protease(s) containing a X-Pro/Ala peptide sequence in its/their N-terminus. *In silico* analyses revealed that SerpinA3N, a serine protease inhibitor, could be a possible candidate for such an enzyme. A previous study demonstrated that SerpinA3N inhibits activity of cathepsin-G, as well [17]. To test this hypothesis, we examined the association between the activity of DPP-4, cathepsin-G, and SerpinA3N using *in vitro* assays. The activity of cathepsin-G was significantly suppressed by SerpinA3N, and was restored by the presence of DPP-4 (Figure 4B). We also found that the inhibitory potential of SerpinA3N against the Granzyme B enzymatic activity was significantly stronger in the absence of DPP-4 (Figure 4C). Taken

together, these results suggest that DPP-4 increases cathepsin-G activity possibly through suppression of SerpinA3N activity in EAM hearts (Figure 4D).

Linagliptin increases SerpinA3N activity in EAM hearts

An ELISA of myocardial lysates revealed that treatment with linagliptin does not affect protein levels of SerpinA3N, although the amount of SerpinA3N was significantly elevated in EAM hearts (Figure 5A). We next evaluated the activity of SerpinA3N in EAM myocardial tissues by an *in vitro* Granzyme B enzymatic activity assay and found that the activity of recombinant Granzyme B was significantly suppressed by lysates of linagliptin-treated EAM myocardial tissues when compared to those of untreated ones (Figure 5B). These results suggest that linagliptin promotes SerpinA3N activity in EAM hearts by inhibiting DPP-4 activity.

DPP-4 upregulates angiotensin II in EAM hearts

Previous investigations have revealed that the renin-angiotensin system plays detrimental roles in the progression of EAM [18-20]. Because cathepsin-G is an alternative enzyme that promotes angiotensin II production from angiotensinogen and/or angiotensin I (Figure 5C), DPP-4-mediated cathepsin-G activation should aggravate EAM by elevating the amount of angiotensin II in myocardial tissues. Consistent with this hypothesis, left ventricular systolic function was significantly higher in EAM hearts treated with losartan, an AT1R antagonist, than in untreated ones after 21 days of EAM induction and cardiac fibrosis after EAM induction was significantly decreased by treatment with losartan (Figure 5D). As it has been shown that SerpinA3N also catalyze chymase [21], we examined the effect of linagliptin on the chymase activity in EAM hearts and found that the activity of chymase in EAM hearts was significantly elevated and linagliptin treatment markedly suppressed the chymase activity (Figure 5E). Expression levels of angiotensin II were significantly elevated in EAM hearts; conversely, expression levels were suppressed by linagliptin treatment (Figure 5F).

These results suggest that DPP-4 upregulates angiotensin II in EAM hearts, possibly through enhancement of cathepsin-G activity.

Linagliptin suppresses oxidative stress in EAM hearts

To examine whether linagliptin, a *xanthine*-based DPP-4 inhibitor, could attenuate oxidative stress in EAM hearts, levels of oxidative stress in the myocardium were determined. The amount of hydrogen peroxide (H_2O_2) in EAM hearts was significantly elevated compared to those in control; moreover, H_2O_2 amounts in EAM hearts were significantly suppressed by linagliptin treatment (Figure 6A). Similarly, the number of 8-OHdG-positive cells in the nuclei, a marker of oxidative stress in cellular DNA, was significantly higher in EAM hearts than those in control, and the number of 8-OHdG-positive cells was significantly decreased by linagliptin treatment (Figure 6B). These results suggest that the beneficial effects of linagliptin on EAM hearts are partially mediated through inhibition of oxidative stress.

Discussion

Previous reports have shown that administration of linagliptin attenuates myocardial inflammation by suppressing cardiac fibrosis, abrogating oxidative stress, and reducing inflammatory cytokine gene expression in mice [12, 22]. In the present study, we revealed a novel mechanism to attenuate autoimmune myocarditis by linagliptin administration (Fig. 7). We determined that DPP-4 physically interacts with cathepsin-G, thereby enhancing intramyocardial cathepsin-G activity by suppressing SerpinA3N. We also found that linagliptin reduces the amount of angiotensin II, a substrate of cathepsin-G, which could be responsible for the aggravation of EAM.

Unbiased comprehensive proteomic analyses with validation assays revealed an association between DPP-4 and cathepsin-G. As stated above, we identified that DPP-4 protects cathepsin-G by inhibiting SerpinA3N activity, using both *in silico* and *in vitro* analyses. Increasing lines of evidence suggest that cathepsin-G, a serine protease that principally locates in azurophilic granules of myeloid cells, plays important roles in the development of inflammation by promoting immune cell migration and activating chemokines [23, 24]. Additionally, it is well known that cathepsin-G participates in the pathogenesis of various autoimmune disorders, such as rheumatoid arthritis, systemic lupus erythematosus, and autoimmune diabetes [25–27]. Consistently, we demonstrated that cathepsin-G activity in EAM hearts was significantly elevated, and that administration of linagliptin attenuated immune cell migration and cathepsin-G activity in the myocardium. To explore in more detail how cathepsin-G is associated with the pathogenesis of EAM, we focused on the role of angiotensin II, one of the major substrates of cathepsin-G, in the progression of EAM. A growing body of evidence suggests that activation of the renin-angiotensin system causes an increase in the release of pro-inflammatory cytokines/chemokines and production of reactive oxygen species, thereby leading to inflammation and development of autoimmune diseases. Indeed, previous studies have shown that suppression of the renin-angiotensin system by treatment with an ACE inhibitor, AT1R blocker, and renin inhibitor effectively alleviates cardiac dysfunction caused by EAM [18–20]. Thus, suppression of cathepsin-G, which catalyzes angiotensin II production from angiotensinogen and/or angiotensin I, should be an effective target for the suppression of EAM activity. Consistently, we here demonstrate that suppression of DPP-4 by linagliptin effectively suppressed angiotensin II levels in EAM hearts. Taken together, our current data suggest that suppression of cathepsin-G activity via DPP-4 inhibition could be a reasonable therapeutic strategy for EAM hearts.

A vast number of previous pre-clinical studies demonstrated that DPP-4 inhibitors play beneficial roles in the progression of cardiovascular diseases, including heart failure. For example, administration of DPP-4 inhibitors improves diastolic failure in diabetic rats, possibly by maintaining blood levels of chemokine stromal cell-derived factor-1, which is a DPP-4 substrate [28]. Administration of DPP-4 inhibitors to a post-cardiac infarction heart failure model showed significant improvement in cardiac function through activation of protein kinase A and promotion of angiogenesis in the myocardium [29]. Thus, DPP-4 inhibitors are expected to be potent therapeutic agents against heart failure.

On the other hand, four cardiovascular outcome trials have been done (the EXAMINE trial with alogliptin [30], the SAVOR-TIMI 53 trial with saxagliptin [31], the TECOS trial with sitagliptin [32], and the CARMELINA trial with linagliptin) [33], but none of them demonstrated the utility of DPP-4 inhibitors on overall heart failure, despite our expectations. Rather, the SAVOR-TIMI 53 trial showed that hospitalizations due to heart failure in diabetic patients that received saxagliptin increased by 27% compared to patients who received the placebo. Thus, there is a discrepancy between the effects of DPP-4 inhibitors in pre-clinical trials and those in clinical trials. However, when a clinical state is appropriately selected, it is considered that DPP-4 inhibitors could be useful for treatment of heart failure. Especially, because DPP-4 has a role on the suppression of the immune system, it may useful for inflammation-based heart failure. Thus, DPP-4 inhibitors may an effective treatment strategy for inflammation-mediated heart failure, such as myocarditis and cardiac sarcoidosis.

It has been shown that linagliptin is a unique DPP-4 inhibitor that may exert anti-oxidant effects, because it has a xanthine-based molecular structure [34, 35]. Oxidative stress plays an important role in the progression of EAM [36]. Our current study demonstrated that the levels of H_2O_2 in the myocardium and the number of 8-OHdG-positive cells decreased following linagliptin treatment. This suggests a beneficial effect of linagliptin on EAM that may be mediated by suppressing oxidative stress, a quality that no other DPP-4 inhibitor may have.

Conclusion

We confirmed that inhibition of DPP-4 by linagliptin is an effective strategy to relieve the disease status of EAM. We also describe a novel mechanism of immunosuppression that is different from the conventionally known mechanisms. Although the results of existing clinical trials have not shown the beneficial effects of DPP-4 inhibitors in heart failure, administration of DPP-4 inhibitors has a potential for clinical applications as a new therapeutic strategy for the treatment of inflammation-mediated heart diseases.

Abbreviations

DPP-4: Dipeptidyl peptidase-4; EAM:Experimental autoimmune myocarditis; GLP-1:Glucagon-like peptide-1; GIP:Glucose-dependent insulintropic polypeptide; CD26:Cluster of differentiation 26; α-MyHC:α-Myosin heavy chain; LVDd:Left ventricular end-diastolic dimension; LVDs:Left ventricular end-systolic dimension; LVFS:Left ventricular fractional shortening; HE:Hematoxylin and eosin; RORγt:RAR-related orphan nuclear receptor gamma; 8-OHdG:8-hydroxyguanosine; TMT:Tandem Mass Tag; LC-MS/MS:Liquid Chromatography / Mass Spectrometry; H_2O_2:Hydrogen peroxide; ELISA:Enzyme-Linked Immuno Sorbent Assay.

Declarations

Availability of data and materials

All data are provided and available in this manuscript.

Ethics approval and consent to participate

All animal care and experimental procedures in this study were approved by the Tokyo Medical and Dental University Guide for the Care and Use of Laboratory Animals (permit number: A2020-043C) and by the Guide for the Care and Use of Laboratory Animals published by the US National Institutes of Health.

Consent for publication

Not applicable.

Competing interests

All of other authors have reported that they have no relationships relevant to the contents of this paper to disclose.

Funding

This work was supported in part by a grant from Boehringer Ingelheim and JSPS KAKENHI Grant-in-Aid for Scientific Research (C) (17K09570 to Y.M.). Dr. Maejima has received speaker honoraria from AstraZeneca, Bayer, Boehringer Ingelheim and received research support from AstraZeneca, Boehringer Ingelheim, Bayer, Bristol-Myers Squibb, Chugai Pharmaceuticals, Eli Lilly, MSD, Novartis Pharma and Taisho-Tomiyama Pharmaceuticals.

Authors’ contributions

YM and YSW: Conception; YSW, YM, SN, NT, TK: Data collection; YSW, YM, SN, NT, TK: Data analysis; YM, YSW and TS: drafting of the manuscript, revision of the manuscript. All authors read and approved the final manuscript.

Acknowledgements

We would like to thank Ms. Noriko Tamura for excellent technical assistance. We also thank Boehringer Ingelheim for providing linagliptin.

References

1. Maisch B, Pankuweit S. Current treatment options in (peri)myocarditis and inflammatory cardiomyopathy. Herz. 2012;37(6):644–56.
2. Feldman AM, McNamara D. Myocarditis. N Engl J Med. 2000;343(19):1388–98.
3. Johnson DB, Balko JM, Compton ML, Chalkias S, Gorham J, Xu Y, Hicks M, Puzanov I, Alexander MR, Bloomer TL, et al. Fulminant Myocarditis with Combination Immune Checkpoint Blockade. N Engl J Med. 2016;375(18):1749–55.
4. Salem JE, Manouchehri A, Moey M, Lebrun-Vignes B, Bastarache L, Pariente A, Gobert A, Spano JP, Balko JM, Bonaca MP, et al. Cardiovascular toxicities associated with immune checkpoint inhibitors: an observational, retrospective, pharmacovigilance study. Lancet Oncol. 2018;19(12):1579–89.
5. Proost P, Struyf S, Schols D, Opdenakker G, Sozzani S, Allavena P, Mantovani A, Augustyns K, Bal G, Haemers A, et al. Truncation of macrophage-derived chemokine by CD26/ dipeptidyl-peptidase IV beyond its predicted cleavage site affects chemotactic activity and CC chemokine receptor 4 interaction. J Biol Chem. 1999;274(7):3988–93.
6. Zhong J, Maiseyeu A, Davis SN, Rajagopalan S. DPP4 in cardiometabolic disease: recent insights from the laboratory and clinical trials of DPP4 inhibition. Circ Res. 2015;116(8):1491–504.
7. Bengsch B, Seigel B, Flecken T, Wolanski J, Blum HE, Thimme R. Human Th17 cells express high levels of enzymatically active dipeptidylpeptidase IV (CD26). J Immunol. 2012;188(11):5438–47.
8. Zhong J, Rao X, Deiuliis J, Braunstein Z, Narula V, Hazey J, Mikami D, Needleman B, Satoskar AR, Rajagopalan S. A potential role for dendritic cell/macrophage-expressing DPP4 in obesity-induced visceral inflammation. Diabetes. 2013;62(1):149–57.
9. Fuchs H, Binder R, Greischel A. Tissue distribution of the novel DPP-4 inhibitor BI 1356 is dominated by saturable binding to its target in rats. Biopharm Drug Dispos. 2009;30(5):229–40.
10. Darsalia V, Ortsater H, Olverling A, Darlof E, Wolbert P, Nystrom T, Klein T, Sjoholm A, Patrone C. The DPP-4 inhibitor linagliptin counteracts stroke in the normal and diabetic mouse brain: a comparison with glimepiride. Diabetes. 2013;62(4):1289–96.
11. Kanasaki K, Shi S, Kanasaki M, He J, Nagai T, Nakamura Y, Ishigaki Y, Kitada M, Srivastava SP, Koya D. Linagliptin-mediated DPP-4 inhibition ameliorates kidney fibrosis in streptozotocin-induced diabetic mice by inhibiting endothelial-to-mesenchymal transition in a therapeutic regimen. Diabetes. 2014;63(6):2120–31.
12. Hirakawa H, Zempo H, Ogawa M, Watanabe R, Suzuki J, Akazawa H, Komuro I, Isobe M. A DPP-4 inhibitor suppresses fibrosis and inflammation on experimental autoimmune myocarditis in mice. PLoS One. 2015;10(3):e0119360.
13. Ito Y, Maejima Y, Tamura N, Shiheido-Watanabe Y, Konishi M, Ashikaga T, Hirao K, Isobe M. Synergistic effects of HMG-CoA reductase inhibitor and angiotensin II receptor blocker on load-induced heart failure. FEBS Open Bio. 2018;8(5):799–816.
14. Ratcliffe NR, Hutchins J, Barry B, Hickey WF. Chronic myocarditis induced by T cells reactive to a single cardiac myosin peptide: persistent inflammation, cardiac dilatation, myocardial scarring and continuous myocyte apoptosis. J Autoimmun. 2000;15(3):359–67.

15. Kanemitsu H, Takai S, Tsuneyoshi H, Nishina T, Yoshikawa K, Miyazaki M, Ikeda T, Komeda M. Chymase inhibition prevents cardiac fibrosis and dysfunction after myocardial infarction in rats. Hypertens Res. 2006;29(1):57–64.
16. Kodama M, Matsumoto Y, Fujiwara M. In vivo lymphocyte-mediated myocardial injuries demonstrated by adoptive transfer of experimental autoimmune myocarditis. Circulation. 1992;85(5):1918–26.
17. Horvath AJ, Irving JA, Rossjohn J, Law RH, Bottomley SP, Quinsey NS, Pike RN, Coughlin PB, Whisstock JC. The murine orthologue of human antichymotrypsin: a structural paradigm for clade A3 serpins. J Biol Chem. 2005;280(52):43168–78.
18. Godsel LM, Leon JS, Wang K, Fornek JL, Molteni A, Engman DM. Captopril prevents experimental autoimmune myocarditis. J Immunol. 2003;171(1):346–52.
19. Liu X, Zhu X, Wang A, Fan H, Yuan H. Effects of angiotensin-II receptor blockers on experimental autoimmune myocarditis. Int J Cardiol. 2009;137(3):282–8.
20. Takamura C, Suzuki J, Ogawa M, Watanabe R, Tada Y, Maejima Y, Akazawa H, Komuro I, Isobe M. Suppression of murine autoimmune myocarditis achieved with direct renin inhibition. J Cardiol. 2016;68(3):253–60.
21. Wagsater D, Johansson D, Fontaine V, Vorkapic E, Backlund A, Razuvaev A, Mayranpaa MI, Hjerpe C, Caidahl K, Hamsten A, et al. Serine protease inhibitor A3 in atherosclerosis and aneurysm disease. Int J Mol Med. 2012;30(2):288–94.
22. Aroor AR, Habibi J, Kandikattu HK, Garro-Kacher M, Barron B, Chen D, Hayden MR, Whaley-Connell A, Bender SB, Klein T, et al. Dipeptidyl peptidase-4 (DPP-4) inhibition with linagliptin reduces western diet-induced myocardial TRAF3IP2 expression, inflammation and fibrosis in female mice. Cardiovasc Diabetol. 2017;16(1):61.
23. Richter R, Bistrian R, Escher S, Forssmann WG, Vakili J, Henschler R, Spodsberg N, Frimpong-Boateng A, Forssmann U. Quantum proteolytic activation of chemokine CCL15 by neutrophil granulocytes modulates mononuclear cell adhesiveness. J Immunol. 2005;175(3):1599–608.
24. Nufer O, Corbett M, Walz A. Amino-terminal processing of chemokine ENA-78 regulates biological activity. Biochemistry. 1999;38(2):636–42.
25. Miyata J, Tani K, Sato K, Otsuka S, Urata T, Lkhagvaa B, Furukawa C, Sano N, Sone S. Cathepsin G: the significance in rheumatoid arthritis as a monocyte chemoattractant. Rheumatol Int. 2007;27(4):375–82.
26. Tamiya H, Tani K, Miyata J, Sato K, Urata T, Lkhagvaa B, Otsuka S, Shigekiyo S, Sone S. Defensins- and cathepsin G-ANCA in systemic lupus erythematosus. Rheumatol Int. 2006;27(2):147–52.
27. Zou F, Lai X, Li J, Lei S, Hu L. Downregulation of cathepsin G reduces the activation of CD4 + T cells in murine autoimmune diabetes. Am J Transl Res. 2017;9(11):5127–37.
28. Shigeta T, Aoyama M, Bando YK, Monji A, Mitsui T, Takatsu M, Cheng XW, Okumura T, Hirashiki A, Nagata K, et al. Dipeptidyl peptidase-4 modulates left ventricular dysfunction in chronic heart failure via angiogenesis-dependent and -independent actions. Circulation. 2012;126(15):1838–51.

29. Birnbaum Y, Castillo AC, Qian J, Ling S, Ye H, Perez-Polo JR, Bajaj M, Ye Y. Phosphodiesterase III inhibition increases cAMP levels and augments the infarct size limiting effect of a DPP-4 inhibitor in mice with type-2 diabetes mellitus. Cardiovasc Drugs Ther. 2012;26(6):445–56.
30. White WB, Cannon CP, Heller SR, Nissen SE, Bergenstal RM, Bakris GL, Perez AT, Fleck PR, Mehta CR, Kupfer S, et al. Alogliptin after acute coronary syndrome in patients with type 2 diabetes. N Engl J Med. 2013;369(14):1327–35.
31. Scirica BM, Bhatt DL, Braunwald E, Steg PG, Davidson J, Hirshberg B, Ohman P, Frederich R, Wiviott SD, Hoffman EB, et al. Saxagliptin and cardiovascular outcomes in patients with type 2 diabetes mellitus. N Engl J Med. 2013;369(14):1317–26.
32. Green JB, Bethel MA, Armstrong PW, Buse JB, Engel SS, Garg J, Josse R, Kaufman KD, Koglin J, Korn S, et al. Effect of Sitagliptin on Cardiovascular Outcomes in Type 2 Diabetes. N Engl J Med. 2015;373(3):232–42.
33. Rosenstock J, Perkovic V, Johansen OE, Cooper ME, Kahn SE, Marx N, Alexander JH, Pencina M, Toto RD, Wanner C, et al. Effect of Linagliptin vs Placebo on Major Cardiovascular Events in Adults With Type 2 Diabetes and High Cardiovascular and Renal Risk: The CARMELINA Randomized Clinical Trial. JAMA. 2019;321(1):69–79.
34. Ghatak SB, Patel DS, Shanker N, Srivastava A, Deshpande SS, Panchal SJ. Linagliptin: a novel xanthine-based dipeptidyl peptidase-4 inhibitor for treatment of type II diabetes mellitus. Curr Diabetes Rev. 2011;7(5):325–35.
35. Kroller-Schon S, Knorr M, Hausding M, Oelze M, Schuff A, Schell R, Sudowe S, Scholz A, Daub S, Karbach S, et al. Glucose-independent improvement of vascular dysfunction in experimental sepsis by dipeptidyl-peptidase 4 inhibition. Cardiovasc Res. 2012;96(1):140–9.
36. Okabe TA, Kishimoto C, Hattori M, Nimata M, Shioji K, Kita T. Cardioprotective effects of 3-methyl-1-phenyl-2-pyrazolin-5-one (MCI-186), a novel free radical scavenger, on acute autoimmune myocarditis in rats. Exp Clin Cardiol. 2004;9(3):177–80.

Figures

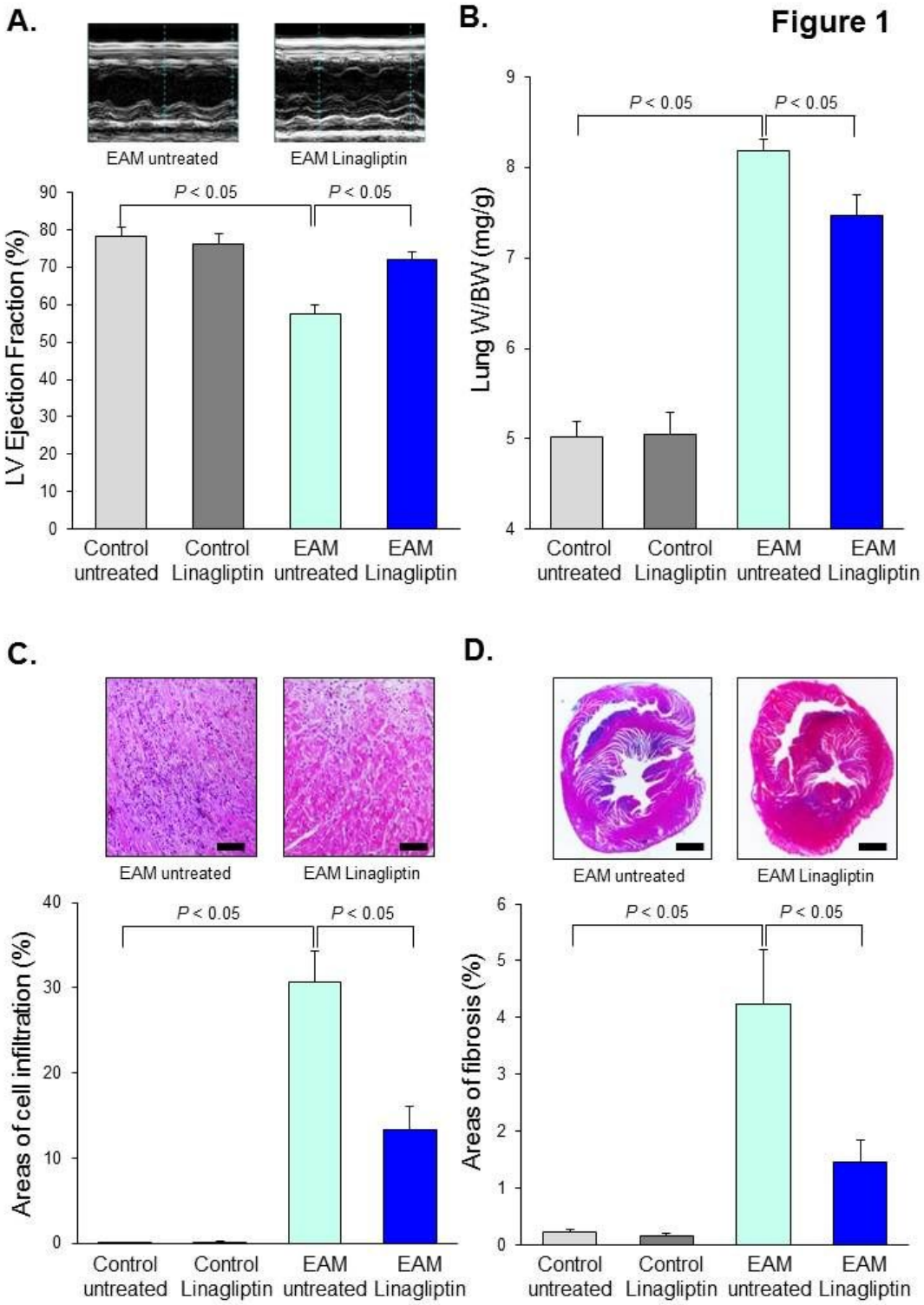

Figure 1

Treatment with linagliptin attenuates inflammatory cell infiltration and fibrosis in EAM hearts A. Representative M-mode echocardiograms and quantitative analyses of LV ejection fraction in EAM mice and linagliptin-administrated EAM mice. P<0.05, n=6. Data are expressed as mean ± SEM. B. Lung weight to body weight ratio in EAM mice and linagliptin-administrated EAM mice. P<0.05, n= 6. Data are expressed as mean ± SEM. C. Representative results of inflammatory cell infiltration and quantitative

analysis of the cell infiltration area in the myocardium of EAM mice and linagliptin-administrated EAM mice. Scale bar: 100 μm, P<0.05, n=6. Data are expressed as mean ± SEM. D. Representative pathological images with Mallory staining in a low power microscopic field and quantitative analysis of the fibrotic area in the myocardium of EAM mice and linagliptin-administrated EAM mice. Scale bar: 2 mm, P<0.05, n=6. Data are expressed as mean ± SEM.

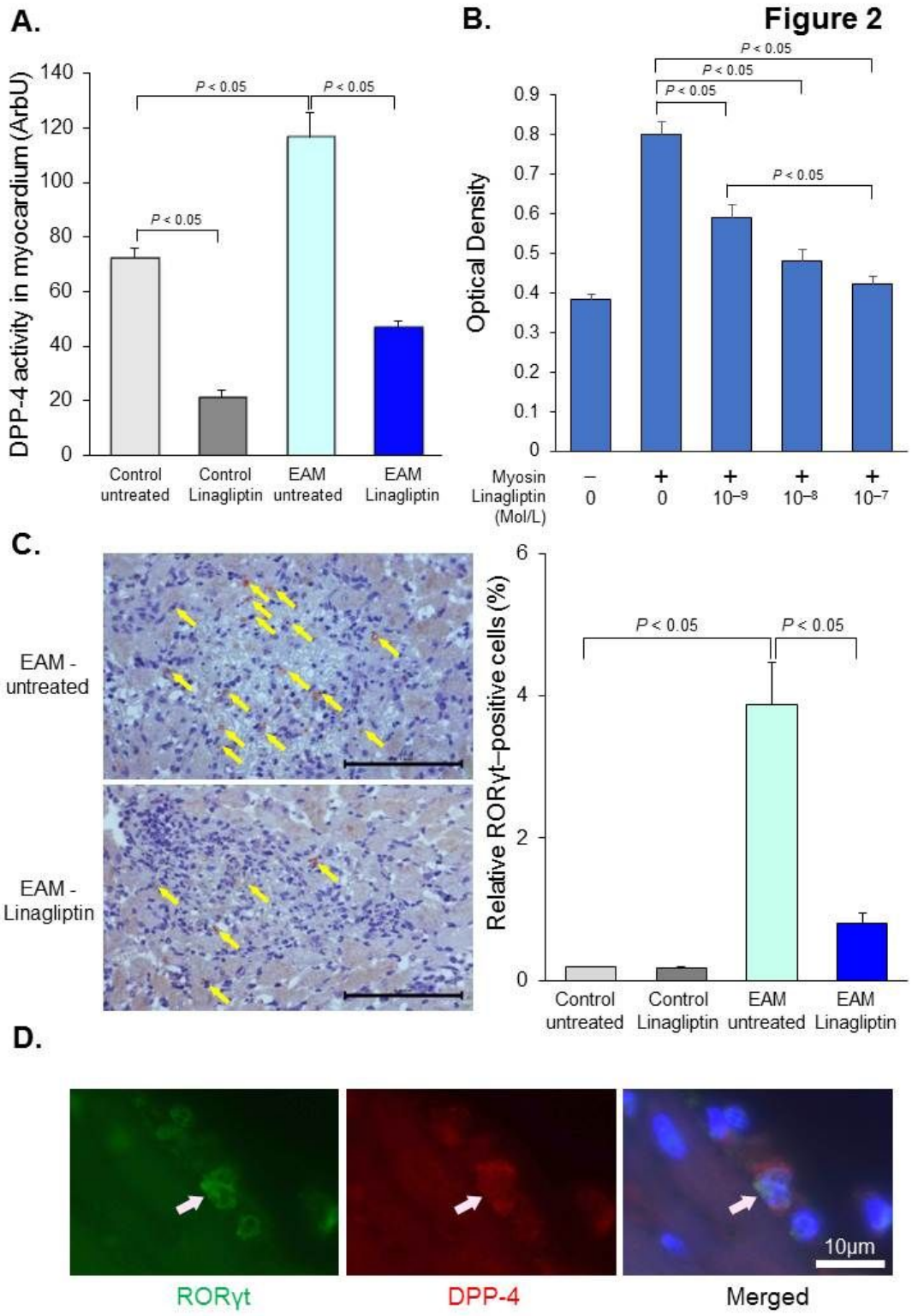

Figure 2

The increase in DPP-4 activity was significantly suppressed by linagliptin treatment in EAM hearts A. Activity of DPP-4 in the myocardium of sham mice, linagliptin-administrated sham mice, EAM mice, and linagliptin-administrated EAM mice. P<0.05, n=6. Data are expressed as mean ± SEM. B. Representative immunostaining and quantitative analysis of RORγt-positive Th17 cells in EAM mice and linagliptin-administrated EAM mice. Arrows indicate RORγt-positive Th17 cells. Scale bar: 100 μm, P<0.05, n=6. Data are expressed as mean ± SEM.

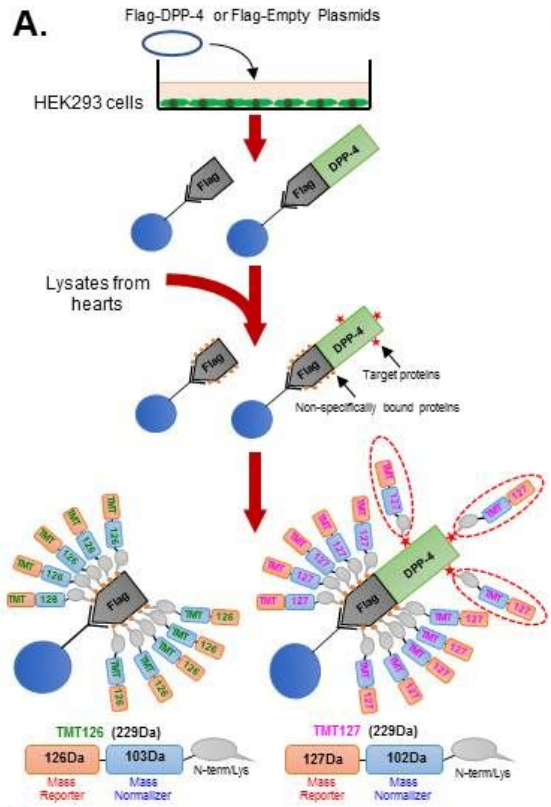

B.

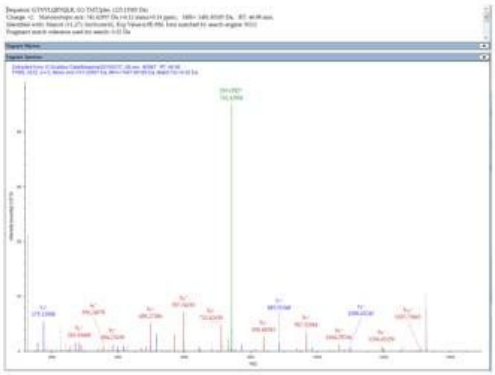

Figure 3

C.

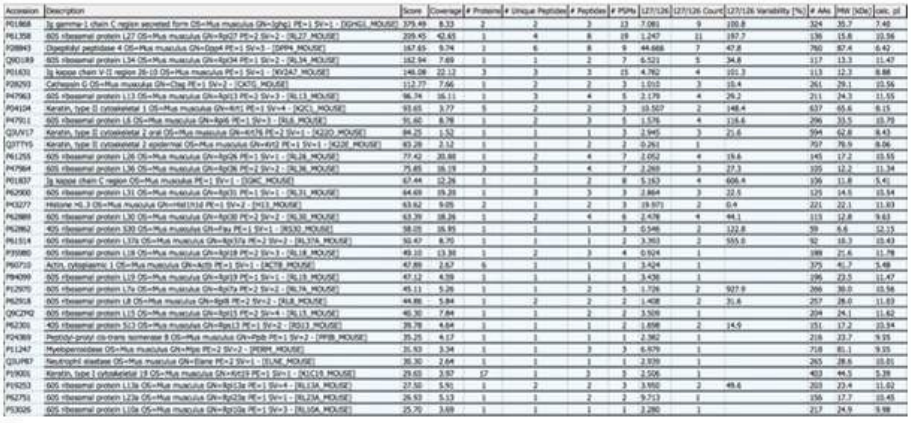

D.

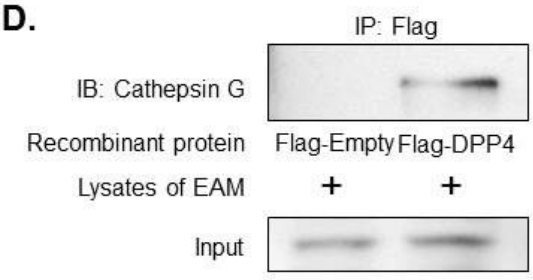

Figure 3

DPP-4 physically interacts with cathepsin-G, a membrane-bound serine protease, in EAM hearts A. Comprehensive analysis for detecting novel proteins that interact with DPP-4 using a Tandem Mass Tag method on mass spectrometric analyses. Flag-DPP-4 or Flag-empty proteins conjugated with magnetic beads via an anti-Flag antibody were immunoprecipitated with lysates from EAM myocardial tissues. Each immunoprecipitate was labeled with a different probe to subtract the signal of nonspecific binding substances. B-C. LC-MS/MS was performed on these samples (B), and data were analyzed to detect the proteins that bind most to DPP-4; peptides were identified by comparing them against the Mus musculus protein database (C). D. Immunoprecipitation analyses of recombinant proteins, flag-empty, and flag-tagged DPP-4.

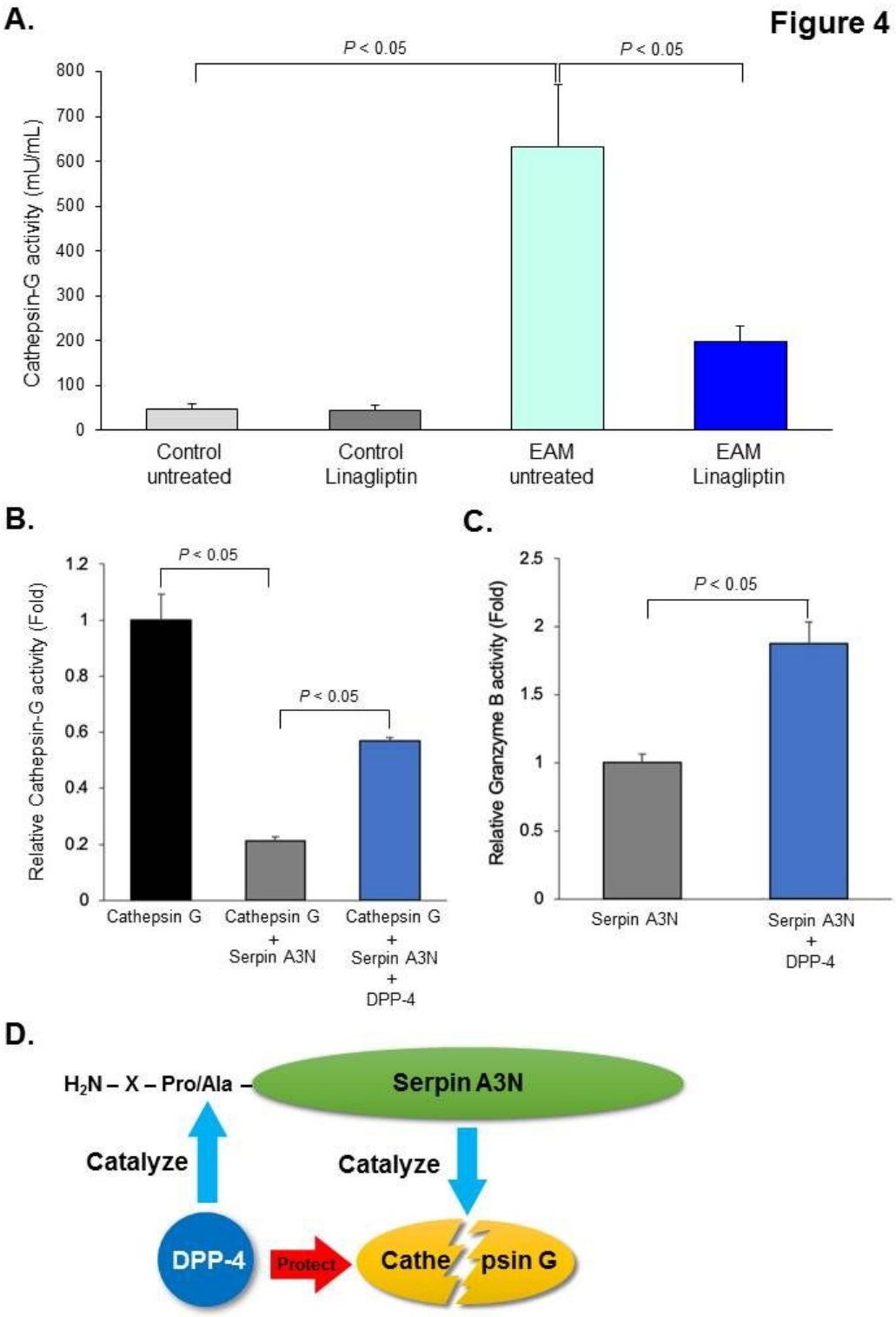

Figure 4

Linagliptin increases SerpinA3N activity in EAM hearts A. Cathepsin G activities in sham mice, EAM mice, and linagliptin-administrated EAM mice. P<0.05, n=6. Data are expressed as mean ± SEM. B. Representative results of immunohistochemistry. Arrows indicate mast cells in myocarditis tissue. C. Cathepsin-G activity in the presence and absence of DPP-4. P<0.05, n=4. D. SerpinA3N activity in the presence and absence of DPP-4. The activity of SerpinA3N was measured by its ability to inhibit

Granzyme B cleavage of tert-butoxycarbonyl-Ala-Ala-Asp-thiobenzyl ester (Boc-AAD-SBzl). P<0.05, n=4. D. Proposed scheme of DPP-4, SerpinA3N, and cathepsin-G. DPP-4 binds to cathepsin-G and inactivates SerpinA3N, which catalyzes cathepsin-G.

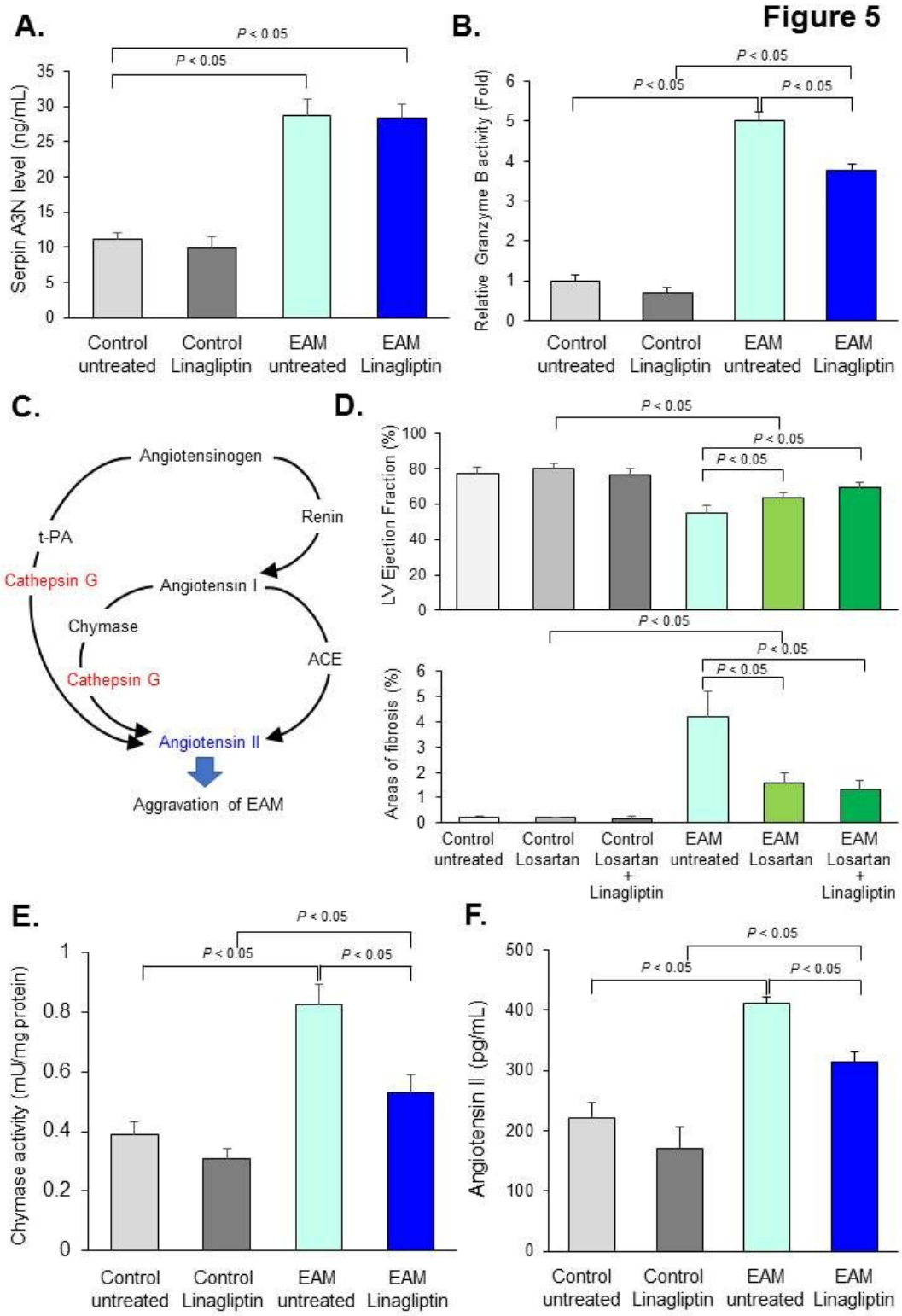

Figure 5

DPP-4 upregulates angiotensin II in EAM hearts A. Protein levels of SerpinA3N in EAM myocardial tissues of sham mice, EAM mice, and linagliptin-administrated EAM mice. P<0.05, n=6. Data are expressed as

mean ± SEM. B. SerpinA3N activity in EAM myocardial tissues of sham mice, EAM mice, and linagliptin-administrated EAM mice. P<0.05, n=6. Data are expressed as mean ± SEM. C. Mechanism of cathepsin G-related angiotensin II generating system. Angiotensin II is generated from a renin-angiotensin system and multiple enzymes such as cathepsin-G. Cathepsin-G can convert angiotensinogen to angiotensin II, and also can directly convert angiotensinogen to angiotensin II. D. The amount of angiotensin II in EAM myocardial tissues of sham mice, EAM mice, and linagliptin-administrated EAM mice. P<0.05, n=6. Data are expressed as mean ± SEM.

Figure 6

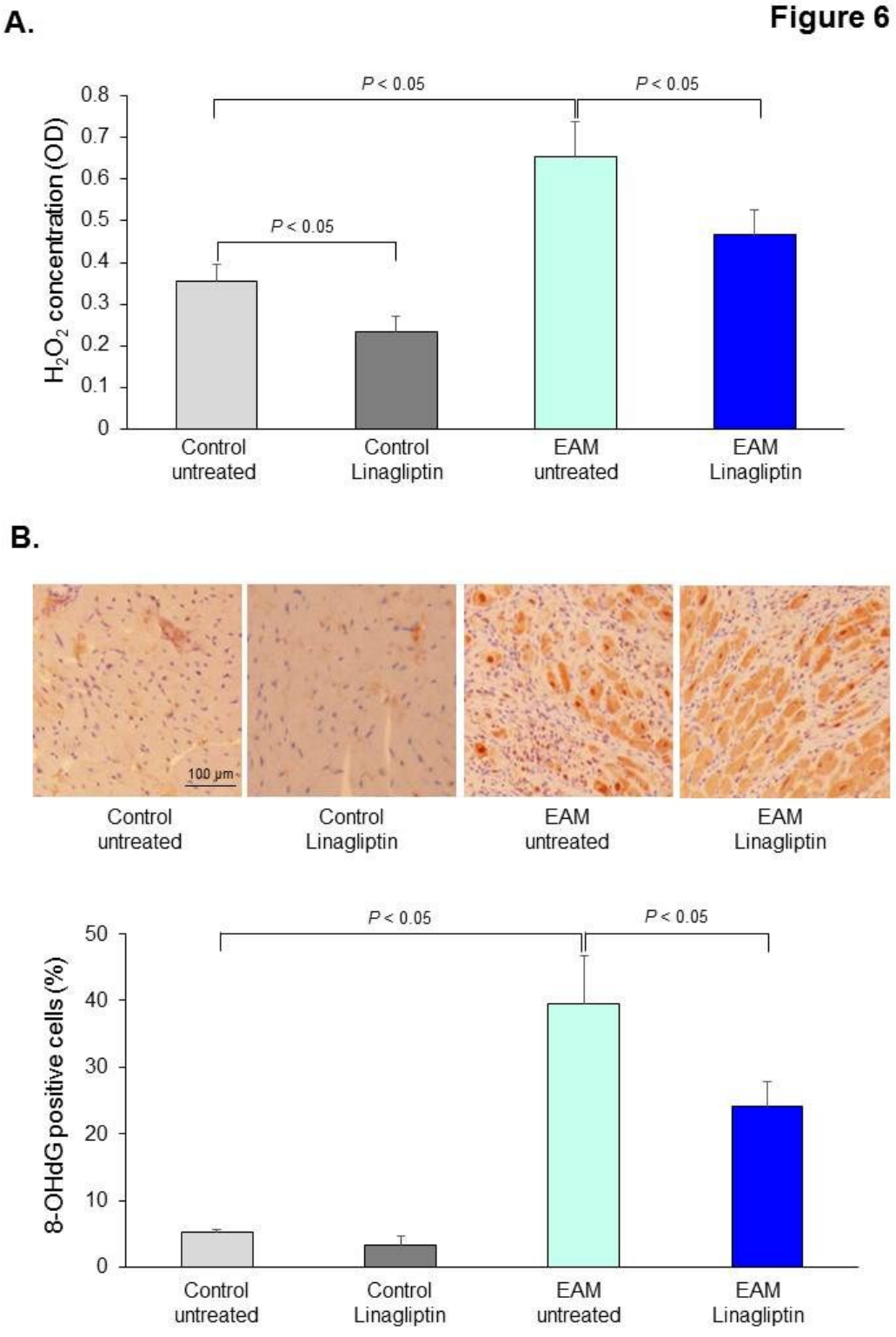

Figure 6

Linagliptin suppresses oxidative stress in EAM hearts A. Hydrogen peroxide (H2O2) concentrations in EAM myocardial tissues of sham mice, EAM mice, and linagliptin-administrated EAM mice on day 21. P<0.05; Control group, n=3; vehicle group, n=5; linagliptin group, n=5. Data are expressed as mean ± SEM. B. Upper: Representative results of immunohistochemistry with 8-hydroguanosine (8-OHdG). Scale bar: 100 μm. Lower: Percentage of 8-OHdG-positive cells in EAM myocardial tissues of sham mice, EAM mice, and linagliptin-administrated EAM mice. n=6 in each group. P<0.05. Data are expressed as mean ± SEM.

Figure 7

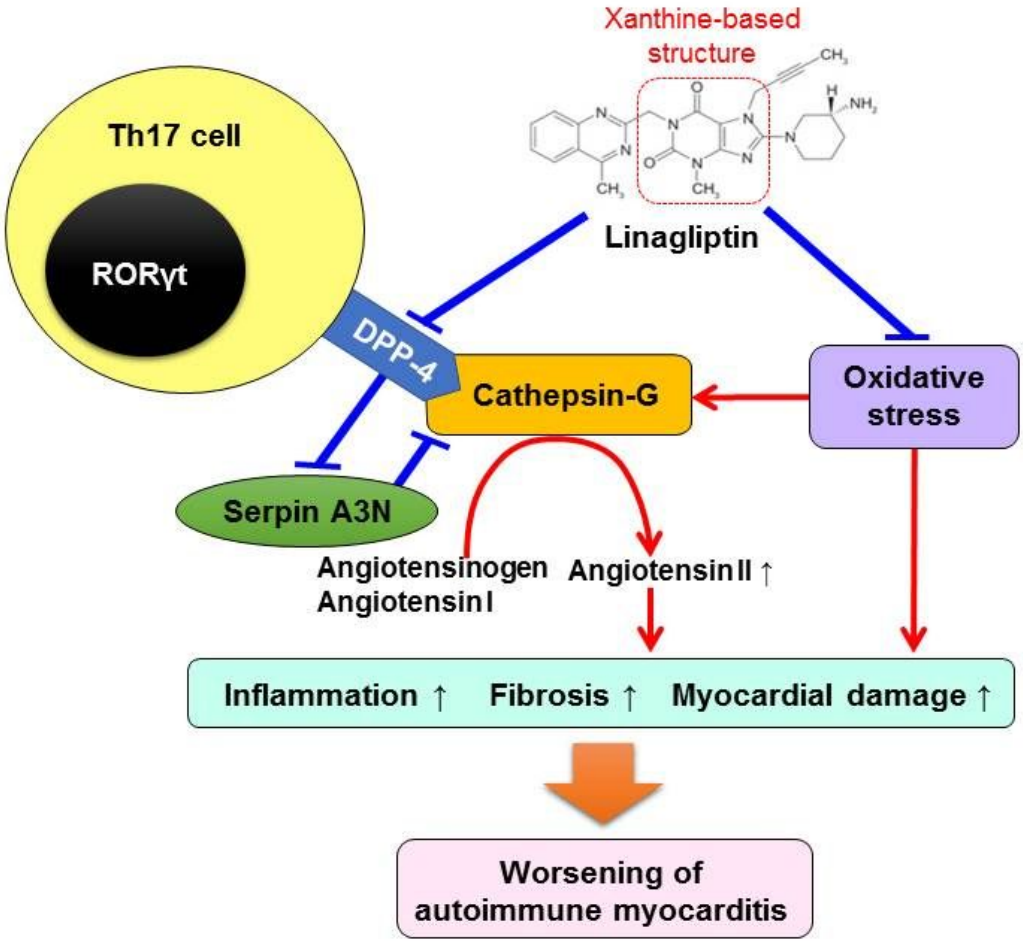

Figure 7

Proposed model for the induction of myocardial damage in EAM by DPP-4 DPP-4 binds to cathepsin-G and protects its activity by inactivating SerpinA3N, which inactivates cathepsin-G. Cathepsin-G converts angiotensinogen and angiotensin I to angiotensin II. Then, Angiotensin II contributes to inflammation, fibrosis, and myocardial damage in EAM.